Spin-dependent bandgap structure and resonant transmission of electrons in ferromagnetic metal/semiconductor cascade junctions

R. L. Zhang, Z. J. Zhang, R. W. Peng,[a] X. Wu, De Li, Jia Li, and L. S. Cao
National Laboratory of Solid State Microstructures and Department of Physics, Nanjing University, Nanjing 210093, People's Republic of China

(Presented on 7 November 2007; received 11 September 2007; accepted 17 October 2007; published online 26 February 2008)

We investigate spin-dependent transport in ferromagnetic metal (FM)/semiconductor (SC) cascade junctions, which can be denoted as $(FM/SC)^n/FM$. Here, n is the repeated number of FM/SC junction. In the Landauer framework of ballistic transport, we have calculated the spin-dependent transmission and the spin polarization in these cascade junctions. It is shown that spin-up and spin-down electrons possess different bandgap structures against the Rashba spin-orbit wave vector. As a result, high spin polarization can be achieved. Besides, resonant transmission for spin-up or spin-down electrons can be observed within the bandgap when we intentionally change the magnetization of FM in the center of the cascade junctions. Around resonant wave vector, spin polarization will be reversed. Our investigations may have potential applications in spin filters and spin switches. © *2008 American Institute of Physics*. [DOI: 10.1063/1.2833756]

In recent years, much attention has been paid to the Datta-Das spin field-effect transistor (SFET),[1] where ferromagnetic metals are used as source and drain contacts (spin injector and detector), and connected to a semiconductor. In the SFET, the spin precession is modulated by Rashba spin-orbit coupling (SOC) in semiconductors.[2] The strength of the Rashba SOC can be tuned by a gate voltage applied on the semiconductor.[3,4] While high spin-injection efficiency can be achieved by using resistive spin-selective contacts and appropriate epitaxial interfaces, in order that spin injects from the ferromagnetic metal (FM) into the semiconductor (SC) and prevails over the conductivity mismatch between these two materials.[5–8] Based on these features, the SFET achieves the potential applications on microelectronic devices.

Quantum interference plays an important role on spin-dependent transport in the SFET.[1,9–14] For example, Shäpers *et al.*[11] have attained an enhanced spin signal by considering the quantum interference effects in the SFET. A quantum spin-valve effect has been found in FM/SC/FM junctions.[12] Switching effect in the SFET and spin filtering in FM/SC/FM/FM heterostructures have also been reported.[13] Therefore, it seems possible to manipulate the spin-polarized transport by designing various FM/SC/FM junctions. In this work, we investigate spin-dependent transport in $(FM/SC)^n/FM$ cascade junctions. Here, n is the repeated number of FM/SC junction. It is shown that spin-up and spin-down electrons possess different bandgap structures against the Rashba spin-orbit wave vector, and high spin polarization can be achieved in some cases. Besides, when we intentionally change the magnetization of FM in the center of the cascade junctions, resonant transmission for spin-up (or spin-down) electrons can be observed within the bandgap.

Suppose that spin transport along the x-axis in a quasi-one-dimensional waveguide, which is composed of the $(FM/SC)^n/FM$ heterojunctions, and electrons are confined in the y-direction by an asymmetric quantum well in the semiconductor, where the Rashba SOC exists. If the width of the transverse confining potential is small enough,[1] we can neglect intersubband mixing. The magnetization of FM layers is chosen along the z direction, which is parallel to the interface. Based on the one-band effective-mass approximation, the Hamiltonians in the FM and SC regions can be written as[14]

$$\hat{H}_f = \frac{1}{2}\hat{p}_x\frac{1}{m_f^*}\hat{p}_x + \frac{1}{2}\Delta\sigma_z \tag{1}$$

and

$$\hat{H}_s = \frac{1}{2}\hat{p}_x\frac{1}{m_s^*}\hat{p}_x + \frac{1}{2\hbar}\sigma_z[\hat{p}_x\alpha_R + \alpha_R\hat{p}_x] + \delta E, \tag{2}$$

respectively. Here, m_f^* and m_s^* are the effective masses of electrons in the FM and SC, respectively. Δ is the exchange splitting energy in the FM, σ_z denotes the spin Pauli matrices, α_R is the spin-orbit Rashba parameter, and δE is the conduction-band mismatch between SC and FM.

Due to the fact that the Hamiltonians shown in Eqs. (1) and (2) are spin diagonal, the electronic eigenstates in the whole $(FM/SC)^n/FM$ system have the form of $|\Psi_\uparrow\rangle = [\psi_\uparrow(x),0]$ and $|\Psi_\downarrow\rangle = [0,\psi_\downarrow(x)]$. In the lth FM/SC cell, the eigenstate in the FM region has the form of

$$\psi_\sigma^{f,l} = A_\sigma^l e^{ik_{F\sigma}^{f,l}(x-x_l)} + B_\sigma^l e^{-ik_{F\sigma}^{f,l}(x-x_l)}, \tag{3}$$

and the eigenstate in the SC region is

$$\psi_\sigma^{s,l} = C_\sigma^l e^{ik_{F,+\sigma}^{s}(x-x_l-d_f/2-d_s/2)} + D_\sigma^l e^{-ik_{F,-\sigma}^{s}(x-x_l-d_f/2-d_s/2)}. \tag{4}$$

Here, x_l is the central position of the FM layer in the lth cell along the x-axis, $\sigma = \uparrow,\downarrow$ indicates spin state of the split band, $k_{F\sigma}^{f,l}$ is the Fermi wave vector in the lth FM layer, $k_{F,\pm\sigma}^{s}$

[a]Author to whom correspondence should be addressed. Electronic mail: rwpeng@nju.edu.cn.

is the Fermi wave vector in the SC layer, and $+\sigma$ (or $-\sigma$) indicates the same (or opposite) spin state with σ. d_f is the thickness of FM layer, d_s is the thickness of SC layer, and we assume the thickness of FM layer or SC layer is invariable in the whole system. At the interface between FM and SC layers, the continuous conditions require

$$\psi_\sigma^f = \psi_\sigma^s, \tag{5}$$

$$\mu \frac{\partial}{\partial x}\psi_\sigma^f = \frac{\partial}{\partial x}\psi_\sigma^s + i\lambda_\sigma K_R \psi_\sigma^s, \tag{6}$$

where $\mu = m_s^*/m_f^*$, $K_R = m_s^* \alpha_R/\hbar^2$, and $\lambda_{\uparrow,\downarrow} = \pm 1$. According to the boundary conditions, the coefficients of A_l, B_l and A_{l+1}, B_{l+1} in two adjacent FM layers are related to a transfer matrix M_1. Suppose N is the total number of FM/SC cells, the global equation for the system can be described as

$$\begin{pmatrix} A_{N+1} \\ B_{N+1} \end{pmatrix} = M \begin{pmatrix} A_1 \\ B_1 \end{pmatrix} = \begin{pmatrix} M_{11} & M_{12} \\ M_{21} & M_{22} \end{pmatrix} \begin{pmatrix} A_1 \\ B_1 \end{pmatrix}, \tag{7}$$

where $M = \prod_{l=1}^{N} M_l$ is the global transfer matrix.[15] The transmission coefficient of the electron with the spin state σ through the whole cascade junctions can be expressed as

$$T_\sigma = \left(\frac{k_{F\sigma}^{f,N+1}}{k_{F\sigma}^{f,1}} \right) \left| \frac{M_{22}M_{11} - M_{12}M_{21}}{M_{22}} \right|^2. \tag{8}$$

Once the spin-dependent transmission coefficient T_σ is achieved, the spin polarization can be calculated by

$$P = (T_\uparrow - T_\downarrow)/(T_\uparrow + T_\downarrow). \tag{9}$$

Based on the above theoretical analysis, we have calculated the spin-dependent transmission coefficient as a function of Rashba spin-orbit wave vector in the $(FM/SC)^n/FM$ heterojunctions for parallel magnetization (as shown in Fig. 1). It is evident that there is no total reflection in the case of small n, although there exist some regions of minimum transmission. When the number of cells becomes larger, total reflection appears at some wave vectors. In general, by increasing the number of cells, more and more transmission zones diminish gradually and some of them approach zero transmission. Therefore, distinct bandgap structure appears in the system. However, the spin-up and spin-down electrons possess different bandgap structures against the Rashba spin-orbit wave vector [as shown in Figs. 1(a)–1(f)]. At some regions of wave vectors, the gap of spin-up electrons can correspond to the band of spin-down electrons. While at other regions of wave vectors, the band of spin-up electrons can overlap with the band of spin-down electrons. Therefore, a spin-dependent bandgap structure is realized in $(FM/SC)^n/FM$ cascade junctions by increasing n.

It is interesting to investigate the spin-polarization effect of the electrons through the $(FM/SC)^n/FM$ cascade junctions. Figure 2 gives the spin polarization against Rashba spin-orbit wave vector in the system with different cell numbers of n. Obviously, the absolute value of spin polarization can be dramatically changed at some wave vectors, which originates from the difference of bandgap structures between spin-up and spin-down electrons. Interestingly, by increasing n, high polarization can be achieved in the $(FM/SC)^n/FM$ cascade junctions. The absolute value of spin polarization can reach 1.0 at some regions of wave vectors when the cell number is large enough. Thereafter, the absolute value of the spin polarization can be changed rapidly from zero to one or from one to zero by increasing the wave vector [for example, as shown in Fig. 2(f)]. This feature provides a way to improve the spin polarization and may have potential applications in the designing of spin switches.

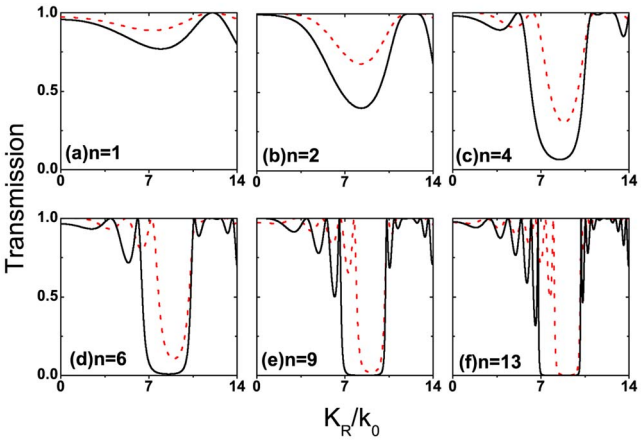

FIG. 1. (Color online) The spin-dependent transmission coefficients as a function of the Rashba spin-orbit wave vector in the $(FM/SC)^n/FM$ cascade junctions with different repeated numbers of cells: (a) $n=1$, (b) $n=2$, (c) $n=4$, (d) $n=6$, (e) $n=9$, and (f) $n=13$. The black solid line and the red dashed one correspond to spin-up and spin-down electrons, respectively. In all calculations in this work, we assume $m_s^*=0.036m_e$, $m_f^*=m_e$, and m_e is the free electron mass. The Fermi wave vectors in the FM for spin-up and spin-down electrons are set as $k_{F\uparrow}=0.44\times10^8$ cm^{-1} and $k_{F\downarrow}=1.05\times10^8$ cm^{-1}, respectively. The conduction-band mismatch between the SC and FM is $\delta E=2.4$ eV. All these calculated parameters are reasonable for Fe- and InAs-based heterostructures (Ref. 13). The thicknesses of FM and SC have been set as $d_f=1$ nm and $d_s=0.1$ μm, respectively. $k_0=1\times10^5$ cm^{-1}, which can be reached in experiments.

Quantum transport in the junctions will be influenced by the impurity-induced scattering. In order to introduce an impurity, we intentionally change the magnetization of FM in the center of the cascade junctions of $(FM/SC)^n/FM$. For example, if the magnetization of FM in the center of junc-

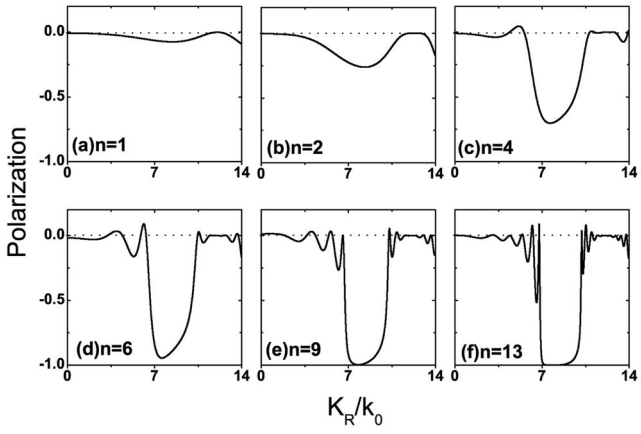

FIG. 2. The spin polarization against the Rashba spin-orbit wave vector in the $(FM/SC)^n/FM$ cascade junctions with different repeated numbers of cells: (a) $n=1$, (b) $n=2$, (c) $n=4$, (d) $n=6$, (e) $n=9$, and (f) $n=13$. The parameters are the same as those in Fig. 1.

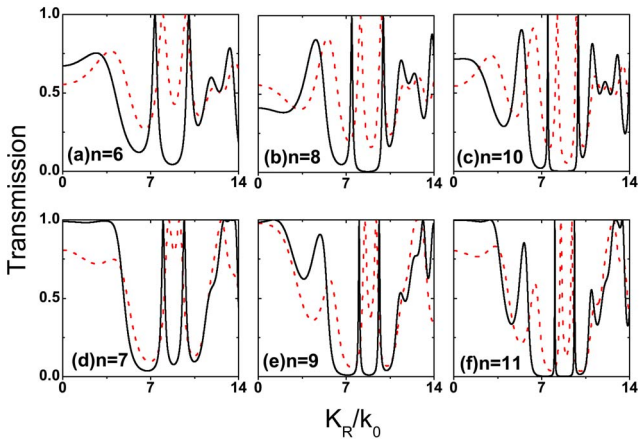

FIG. 3. (Color online) The spin-dependent transmission coefficients as a function of the Rashba spin-orbit wave vector in the $(FM/SC)^n/FM$ cascade junctions, where the magnetization of FM in the central cell is reversed intentionally. When n is even, the magnetization of FM in the $[(n/2+1)]$th cell is reversed. While n is odd, the magnetizations of FM both in the $(n+1)/2$th cell and the $(n+3)/2$th cell are reversed. The number of cells in the cascade junctions is (a) $n=6$, (b) $n=8$, (c) $n=10$, (d) $n=7$, (e) $n=9$, and (f) $n=11$, respectively. The black solid line and the red dashed one correspond to spin-up and spin-down electrons, respectively.

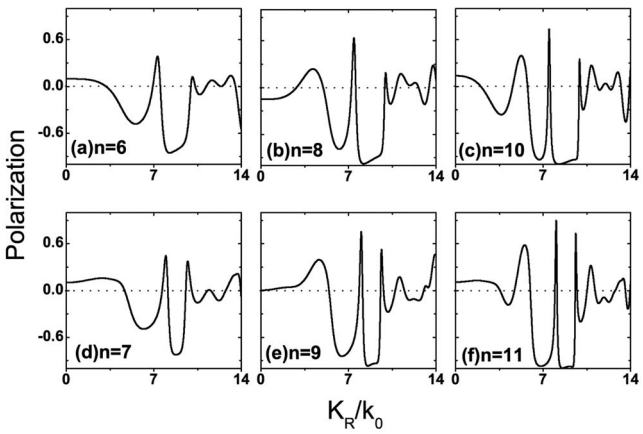

FIG. 4. The spin polarization against the Rashba spin-orbit wave vector in the $(FM/SC)^n/FM$ cascade junctions described in Fig. 3. The number of cells in the cascade junctions is (a) $n=6$, (b) $n=8$, (c) $n=10$, (d) $n=7$, (e) $n=9$, and (f) $n=11$, respectively.

tions is reversed, it acts as an impurity in the whole cascade junctions. Figure 3 shows the transmission coefficients for spin-up and spin-down electrons transmitting through the $(FM/SC)^n/FM$ cascade junctions, where the magnetization of FM in the centre is reversed. There are several interesting features (as shown in Fig. 3). First, there exist perfect transmission peaks within the bandgap for spin-up or spin-down electrons due to the impurity-induced scattering. Second, the resonant wave vectors for spin-up and spin-down electrons are separated because the phase shift between spin-up and spin-down electrons is different when the Rashba SOC strength is modulated. Third, the quality factor of the resonant transmission peak in the bandgap is increased by increasing n, which may come from multiple scatterings of the electron in the cascade junctions. These features may be used to design the spin filters.

It is worthwhile to study the spin-polarization property when we intentionally change the magnetization of FM in the centre of the $(FM/SC)^n/FM$ cascade junctions. As shown in Fig. 4, the spin polarization can be changed alternatively from positive to negative against the Rashba spin-orbit wave vector. Around resonant wave vectors, high spin-polarization has been observed and the spin polarization has been reversed. This feature originates from the fact that resonant wave vectors are spin dependent. Therefore, it becomes possible to control the spin-polarization reversal of tunneling electrons by tuning the Rashba SOC strength with a gate voltage in the cascade junctions. On the other hand, by increasing the cell number of n, the absolute value of spin polarization gradually increases at resonant wave vector [as shown in Figs. 4(a)–4(f)]. The reason is that with increasing the cell number, the resonant transmission peaks become more and more sharper, and the transmission will dramatically decrease once the wave vector is slight deviated from the resonant wave vectors [as shown in Figs. 3(a)–3(f)]. As a result, more and more higher polarization can be achieved around the resonant wave vector by increasing the number of FM/SC cells. Therefore, the spin polarization of tunneling electrons can be reversed by inducing the impurity, such as changing the magnetization of central FM layer, and the spin polarization can also be enlarged by increasing the cell number in the FM/SC cascade junctions.

This work was supported by the grants from National Natural Science Foundation of China (10625417, 50672035, and 90601001), the State Key Program for Basic Research from the Ministry of Science and Technology of China (2004CB619005 and 2006CB921804), and partly by the Ministry of Education of China (NCET-05-0440).

[1] S. Datta and B. Das, Appl. Phys. Lett. **56**, 665 (1990).
[2] E. I. Rashba, Sov. Phys. Solid State **2**, 1190 (1960).
[3] J. Nitta, T. Akazaki, H. Takayanagi, and T. Enoki, Phys. Rev. Lett. **78**, 1335 (1997).
[4] D. Grundler, Phys. Rev. Lett. **84**, 6074 (2000).
[5] E. I. Rashba, Phys. Rev. B **62**, R16267 (2000); G. Kirczenow, *ibid.* **63**, 054422 (2001); S. F. Alvarado, Phys. Rev. Lett. **75**, 513 (1995); H. Ohno, Science **281**, 951 (1998).
[6] V. Delmouly, A. Bournel, G. Tremblay, and P. Hesto, *Abstracts of the Symposium on Spin-Electronics* (Halle, Germany, 2000).
[7] A. T. Hanbicki *et al.*, Appl. Phys. Lett. **82**, 4092 (2003).
[8] X. Jiang *et al.*, Phys. Rev. Lett. **94**, 056601 (2005).
[9] X. F. Wang, P. Vasilopoulis, and F. M. Peeters, Appl. Phys. Lett. **80**, 1400 (2002).
[10] J. C. Egues, G. Burkard, and D. Loss, Phys. Rev. Lett. **89**, 176402 (2002).
[11] Th. Schäpers, J. Nitta, H. B. Heersche, and H. Takayanagi, Phys. Rev. B **64**, 125314 (2001).
[12] F. Mireles and G. Kirczenow, Phys. Rev. B **66**, 214415 (2002).
[13] Y. Guo, X.-W. Yu, and Y.-X. Li, J. Appl. Phys. **98**, 053902 (2005); K. M. Jiang, Z. M. Zheng, B. G. Wang, and D. Y. Xing, Appl. Phys. Lett. **89**, 012105 (2006).
[14] H.-C. Wu, Y. Guo, X.-Y. Chen, and B.-L. Gu, J. Appl. Phys. **93**, 5316 (2003); F. Mireles and G. Kirczenow, Europhys. Lett. **59**, 107 (2002).
[15] R. L. Zhang, R. W. Peng, L. S. Cao, Z. Wang, Z. H. Tang, X. F. Zhang, M. Wang, and A. Hu, Appl. Phys. Lett. **89**, 153114 (2006); R. L. Zhang, R. W. Peng, X. F. Hu, L. S. Cao, X. F. Zhang, M. Wang, A. Hu, and S. S. Jiang, J. Appl. Phys. **99**, 08F710 (2006).